JOURNAL OF MATERIALS SCIENCE 27 (1992) 3379–3388

Analysis and modelling of the die drawing of polymers

S. N. KUKUREKA*, G. CRAGGS†, I. M. WARD
Interdisciplinary Research Centre for Polymer Science and Technology, and † Department of Mechanical Engineering, University of Leeds, LS2 9JT, UK

An analysis of the mechanics of the die-drawing process for polymer orientation has been undertaken on the basis of the lower bound theory by Hoffman and Sachs for metals, with several important modifications. First it is accepted that the flow stress in polymers is strongly dependent on plastic strain, strain rate and temperature. Secondly, thermal effects during die drawing due to heat generated by plastic deformation are included in the analysis. Finally, the temperature distribution in the die is estimated, taking into account both heat condition and axial translation of the polymer during the drawing process. Good agreement was obtained between theoretically predicted drawing stresses and those determined experimentally for a range of drawing speeds.

1. Introduction

1.1. Background information

The die-drawing process is a method of producing highly oriented polymer sections with the material, during processing, being in the solid phase. Usually, a heated polymer billet is drawn through a converging die to produce rod, sheet, tube or mono-filament. The resulting products have enhanced mechanical properties when compared with the starting material, and in particular show considerable increase in strength and stiffness together with improvements in thermal stability, barrier properties and chemical resistance, making them useful in a wide variety of applications.

Die drawing developed from early studies of the tensile drawing of polymers [1–3] and from the hydrostatic extrusion process [4, 5]. Its development route differed from that of fibres where solution and melt processes were used to produce high-modulus materials. A review of the preparation, structure and properties of high-modulus polymers produced by all the above routes has been published [6].

Initial die-drawing work at Leeds was carried out on a small-scale die drawing facility [7–12] but the process has been successfully scaled up and a batch machine has been designed and developed which is capable of producing large-section products in a variety of materials [13, 14]. A continuous die-drawing machine is currently under development. Considerable experimental data have been obtained from these facilities but there is also a need for a fundamental analysis of the process to identify parameters which affect die-drawing behaviour. The aim of this paper is to provide such an analysis, primarily through a computer model, of the die-drawing process applied to polyethylene.

1.2. Die-drawing process

The drawing of a polymer through a die is shown schematically in Fig. 1. Region 1 contains undeformed material moving towards the die entrance while in Region 2 the polymer is deformed within the die whilst remaining in contact with the die wall. Some polymers remain in contact with the die wall throughout the drawing process while others, with particular strain-hardening characteristics, prematurely neck down and leave the die wall as seen in Region 3. A substantial amount of free tensile drawing can occur downstream of the die exit (Region 4) as the polymer cools from its processing temperature and eventually reaches a constant cross-sectional area (Region 5).

In all cases, the nominal draw ratio, R_N, and the actual draw ratio, R_A, are used to quantify the deformation behaviour and these quantities are defined by

$$R_N = \frac{\text{Original billet cross-section area}}{\text{Die exit cross-sectional area}}$$

and

$$R_A = \frac{\text{Original billet cross-sectional area}}{\text{Final product cross-sectional area}}$$

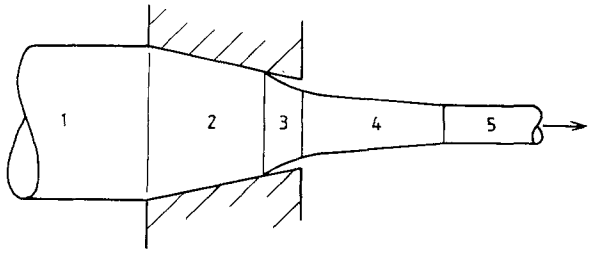

Figure 1 Regions observed when drawing a polymer billet through a converging die.

* *Present address*: School of Metallurgy and Materials, University of Birmingham, Birmingham, UK.

0022-2461

The case of a circular billet being drawn through a conical die having a semi-angle of 15° is analysed theoretically. Attention is focused primarily on Region 2 because the drawing characteristics of any polymer are governed by its behaviour in this region. The analysis applies up to the point where the material leaves the die wall or reaches the die exit. The results obtained are crucially dependent on the flow stress of deforming material within the die and this parameter is greatly affected by strain rate and temperature.

2. Principles of the die-drawing model

The three central elements in the analysis of the process are the mechanics of the process, the yield or flow stress of the material being processed and the thermal effects, because these parameters influence mechanical behaviour. In this work the mechanics of drawing was approached through the equilibrium equation due to Hoffman and Sachs [15] and yield behaviour was deduced using either the Eyring activated rate theory [16] or from experimental uniaxial stress–strain data determined over a range of strain-rates. The temperature distribution in the material during drawing was evaluated using finite difference techniques with the heat generated by mechanical work being taken into account in the calculation.

A solution to the stress field for material within the die was obtained using a numerical iterative procedure which solved the equilibrium equation for individual elements of material taking into account their temperature and their assigned value of flow stress. Elements within the die were obtained by first dividing the length of the die into a number of slices (usually 20–80) by planes normal to the die axis such that each slice was of constant volume. Each slice was then divided radially into annular elements (usually 5) also of constant volume so that a mesh as shown in Fig. 2 was obtained. A solution of the equilibrium equations derived from the mechanics of drawing for each element gave the stresses in the material at these points.

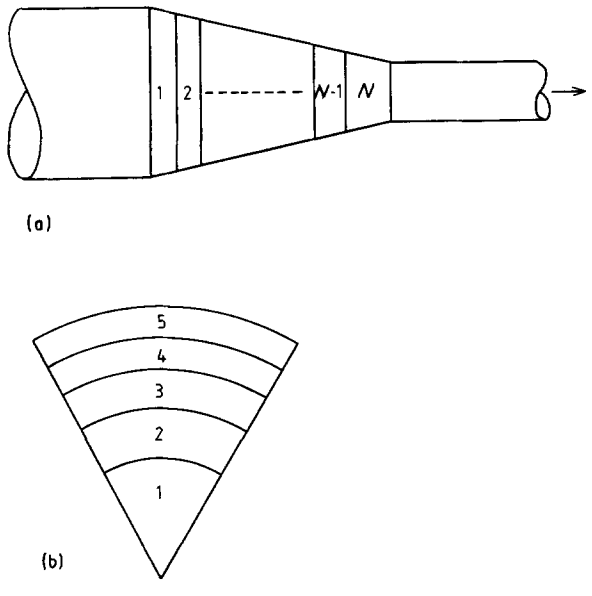

Figure 2 Elements used in the analysis of the die-drawing process. (a) Axial elements. (b) Radial division of each axial element.

3. Mechanics of die drawing

The theory of plastic flow in conical dies was originally developed for the analysis of metal forming processes. The upper bound theory [17] satisfies the continuity requirement but is found to give an over estimate of the forces with the die material. The lower bound theory [15] satisfies equilibrium requirements but not necessarily continuity, and gives a lower limit of the forces and stresses within the material. Coates *et al.* [18] satisfactorily analysed the mechanics of hydrostatic extrusion of polymers using the equilibrium or lower bound theory of Hoffman and Sachs [15] and this approach has been used in the present work.

The lower bound approach is based on the quasi-equilibrium of forces acting on a small element of material within the die. It assumed that plane sections remain plane during drawing and that the axial force does not vary with radius. Avitzur [17] has shown that for dies having a semi-angle less than 15° it is acceptable to assume plug flow and therefore the equilibrium approach of Hoffman and Sachs [15, 18] may be used to determine the stress in an element.

By considering the equilibrium of the forces acting on an element of material, as shown in Fig. 3, it is found that the relationship between the stresses [15] is given by

$$\frac{d\sigma_x}{d\varepsilon} = \sigma_x - \sigma_y(1 + \mu \cot \alpha) \quad (1)$$

where σ_x is the axial stress, σ_y the stress normal to the wall, ε the true axial strain, μ the coefficient of friction between the material and die wall and α the die semi-angle.

Assuming deformation of the material occurs under constant volume conditions, then the true axial strain, ε, may be expressed in terms of the initial and final values of radius of an element

$$\varepsilon = \ln\left(\frac{r_0}{r}\right)^2 \quad (2)$$

Because $d\varepsilon = -(2dr/r)$, Equation 1 becomes

$$d\sigma_x = [\sigma_y(1 + \mu \cot \alpha) - \sigma_x]\frac{2dr}{r} \quad (3)$$

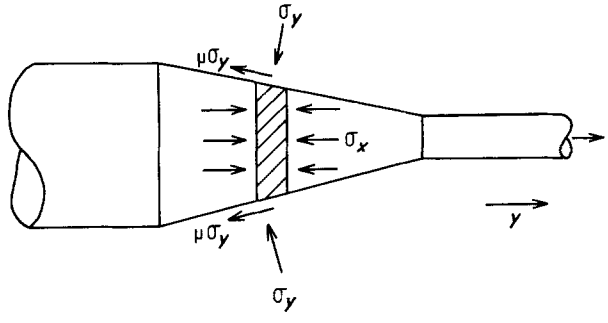

Figure 3 Stresses acting on an axial element within the die.

This equation must be satisfied for all elements in the die but a relationship between σ_x and σ_y is required before the equation may be solved. This may be obtained from the yield behaviour of the material. Although the yield behaviour of polymers is known to be pressure-dependent, it has been found adequate to represent the flow stress in the present case in terms of either the Tresca yield criterion or von Mises yield criterion [18], which give

$$\sigma_f = \sigma_x - \sigma_y \quad (4)$$

where σ_f is the flow stress at an appropriate strain, strain rate, temperature and pressure acting on a given element.

Eliminating σ_y between Equations 3 and 4 gives

$$d\sigma_x = [L\sigma_x - \sigma_f(1 + L)]\frac{2dr}{r} \quad (5)$$

where $L = \mu \cot \alpha$. This equation enables the axial stress to be calculated for any element in the die, provided the yield behaviour of the polymer is known. Implicit in this approach is the assumption that σ_x and σ_y are parallel and normal, respectively, to the draw direction and that they are principal stresses. This is approximately true provided the die angle and the friction coefficient at the die wall are both small. Furthermore, this theory is only valid for material being deformed by the die and will not apply to material which prematurely leaves the die wall and begins to neck down. The point of departure from the die wall can be identified because it must coincide with the value of σ_y being zero or negative.

4. Yield behaviour

The flow stress within the die has been seen to be dependent on stress, strain, strain rate, temperature and hydrostatic pressure although pressure is considered to have negligible effect in the present work. The stresses and strains in the die are triaxial with the axial stress being the dominant stress during drawing. Consequently, the flow stress at any point in the die may be assumed to be the same as that in a tension specimen having the same axial strain, particularly since it may be shown that the equivalent strain is the same in both cases.

Coates and Ward [19] have shown that in uniaxial tension a unique relationship exists between stress, strain and strain rate which is independent of the load path followed by the material. It is therefore possible to deduce the flow stress for any strain, strain rate and temperature situation by interpolation of uniaxial data.

In this work the yield behaviour of the material was determined by two separate routes. In the first, the yield behaviour itself was modelled using the activated rate theory originally developed by Eyring and co-workers [16] and previously applied to the hydrostatic extrusion of polymers [20]. In the second, the experimental stress–strain data from mechanical tests were used as discussed above.

4.1. Activated rate theory

Yielding may be considered to be an activated rate process where deformation of a polymer involves the motion of chain molecules or parts of chain molecules over potential energy barriers. With no stress acting, a dynamic equilibrium exists with chains moving over the potential energy barrier in both directions. This approach [21] leads to the formulation of the equation for strain rate, $\dot{\varepsilon}$, as

$$\dot{\varepsilon} = \dot{\varepsilon}_0 \exp\left(-\frac{\Delta U}{kT}\right) \quad (6)$$

where $\dot{\varepsilon}_0$ is the pre-exponential factor, ΔU the activation energy, T the absolute temperature, and k Boltzmann's constant.

The effect of applying a stress, σ, to the polymer is to shift the energy barrier so that there is a net flow of chain molecules in one direction and because this flow is related to strain rate

$$\dot{\varepsilon} = \dot{\varepsilon}_0 \exp\left[\left(-\frac{\Delta U - \sigma V}{kT}\right)\right] \quad (7)$$

where V is the activation volume. Rearranging this equation gives

$$\sigma = \frac{1}{V}\left[\Delta U + kT \ln\left(\frac{\dot{\varepsilon}}{\dot{\varepsilon}_0}\right)\right] \quad (8)$$

The initial yield stress of a polymer in a state of tension may be predicted from this equation and it may also be used to predict the subsequent flow stress as the strain, strain rate and temperature change during deformation.

When modelling the behaviour of polyethylene, data from Hope and Ward [20] were used; the activation energy was taken to be 180 kJ mol^{-1} and the pre-exponential factor, $\dot{\varepsilon}_0$, was found to decrease with draw ratio from an initial value of 8×10^{19} s^{-1} to 6×10^{19} s^{-1} when the draw ratio reached 6. It could be represented by the equation

$$\ln \dot{\varepsilon}_0 = 45.82 - 0.147 \ln \lambda \quad (9)$$

Equation 8 shows activation volume to have a marked influence on flow stress. Hope and Ward [20] suggest that high strains and strain rates are usually associated with a high stress, low activation volume process while low strains relate to low stress, high activation volume. Their data for polyethylene show a decrease in activation volume from about 7 nm^3 for isotropic material to less than 1.5 nm^3 for draw ratios of 6.

It is possible to take into account the effect of hydrostatic stress on flow stress behaviour by adding an appropriate term to Equation 8. However, this was not necessary in the present work because the hydrostatic stress in the die is relatively small and not expected to influence flow stress to any significant extent. In the present work, Equation 8 was used to evaluate flow stress and the results related to elements of material being deformed within the die.

4.2. Experimental yield data

An alternative way of obtaining yield data from the computer model of the die drawing process is from mechanical tests on the material. It has already been

seen that for a given point within the die, the flow stress will be approximately equal to that in a uniaxial specimen for comparable strain, strain rate and temperature conditions. Values of flow stress within the die can, therefore, be deduced from uniaxial test data.

A series of tensile tests were carried out on plastically deformed polyethylene (BP grade R006-60) tension specimens using an RDP mechanical testing machine. In each test the specimens were enclosed in an environmental chamber and tests carried out at 95 and 100 °C at constant cross-head speed. Strain rate during these tests, therefore, decreased with increasing strain. In contrast, strain rate in the die-drawing process progressively increases with strain reaching a maximum at the die exit. A significant loss of accuracy occurs if tensile test data are related to die drawing based on average strain rates. Rather, flow stress values in the die must be deduced from the point by point correlation of strain and strain rate in a tension specimen. This approach is possible because Coates and Ward [19] have shown that in uniaxial tension a polymer has a unique stress–strain–strain rate–temperature characteristic which is independent of the load path taken to achieve a given mechanical state. Thus, composite flow stress curves relating to the strain and strain rate experienced by an element of material passing through the die for a given draw speed can be deduced from uniaxial data.

To obtain a composite curve, the basic tensile test data were converted to true stress–true strain relationships and true strain rate evaluated throughout each test. A plot of true stress–log (true strain rate) for a given strain in the tensile specimens produced, as expected, a linear relationship as shown in Fig. 4. The axial strain within the die can be determined from Equation 2 and strain rate from the expression

$$\dot{\varepsilon} = \frac{4vd_f^2 \tan\alpha}{d^3} \qquad (10)$$

where v is the product velocity at the die exit, d_f the product diameter, and d the instantaneous diameter.

5. Die-drawing temperature distribution

The mechanical work of deformation during die drawing is capable of producing an increase in temperature and a corresponding reduction in flow stress which could have a significant effect on the drawing behaviour. To take this factor into account, a knowledge of the quasi-steady state temperature distribution in the die was required. This involved estimating the quantity of heat generated within the material due to mechanical work and allowing for heat conduction in the axial and radial directions with the die acting as a heat sink and being maintained at a constant temperature. In the axial direction, the thermal conductivity increases with orientation whereas the radial conductivity remains approximately the same as for isotropic material [22]. In addition, the effects of the material moving through the die must be taken into account together with its changing geometry. A solution to the temperature distribution in this case was obtained by numerical analysis with the deforming polymer subdivided into equal volume elements as shown in Fig. 2, and the temperature of each element adjusted so as to satisfy the heat-conduction equation.

The basic one-dimensional heat-conduction equation for a cylindrical medium moving with velocity, U_x, with internal heat generation f/unit volume of material [23], is given by

$$\frac{\partial^2 T}{\partial x^2} - \frac{U_x}{\nu}\left(\frac{\partial T}{\partial x}\right) + \frac{f}{k} = \frac{1}{\nu}\left(\frac{\partial T}{\partial t}\right) \qquad (11)$$

where T is temperature, t is time, k the thermal conductivity and ν the thermal diffusivity which is related to density, ρ, and specific heat, c, by $\nu = k/\rho c$. When Equation 11 is expressed in finite difference form and applied to the centre element, i shown in Fig. 5a, then the equation to be satisfied becomes

$$\frac{T_{i+1} + T_{i-1} - 2T_i}{(\Delta x)^2} - \lambda_i U_b \frac{\rho c}{k}\left(\frac{T_{i+1} - T_{i-1}}{2\Delta x}\right) + \frac{\lambda_i U_b}{\Delta x}\frac{\sigma_i d\varepsilon_i}{k} = \frac{\rho c}{k}\left(\frac{T_i' - T_i}{\Delta t}\right) \qquad (12)$$

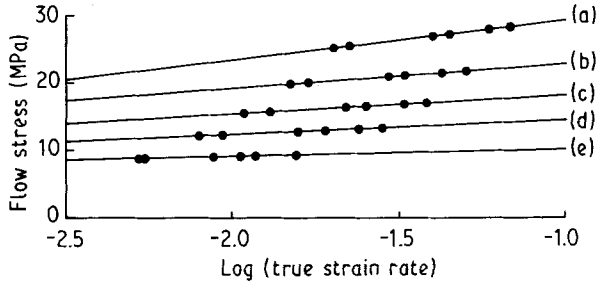

Figure 4 Flow stress–strain rate characteristics of polyethylene R006-60 obtained from tension tests at 100 °C: strain ε = (a) 1.4, (b) 1.2, (c) 1.0, (d) 0.8, (e) 0.4.

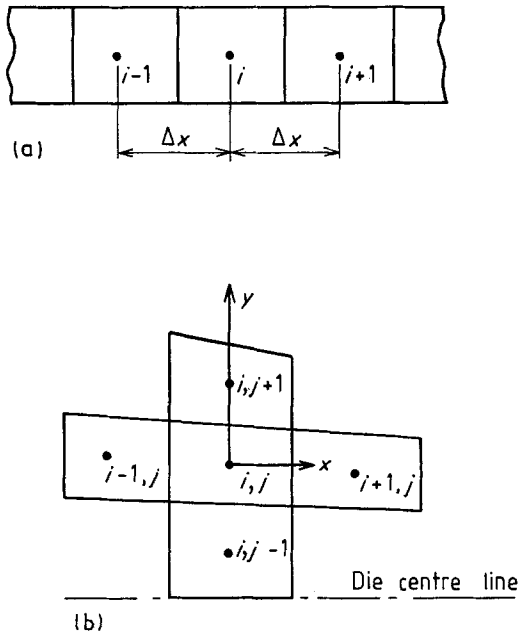

Figure 5 General elements used in heat-conduction analysis. (a) One-dimensional heat conduction. (b) Axial and radial heat conduction within a die.

where λ_i is the current draw ratio of the element and U_b the initial billet velocity. In the heat-generation term, σ_i, is the current flow stress and $d\varepsilon_i$ the increment of plastic strain occurring during time interval Δt. The temperature T'_i of element i after time Δt may be evaluated from Equation 12 and it may be shown that

$$T'_i = T_{i+1}\left(1 - \frac{A\rho c}{2}\right)\Big/M + T_{i-1}\left(1 + \frac{A\rho c}{2}\right)\Big/M + T_i(M - 2)/M + A\sigma_i d\varepsilon_i/M \quad (13)$$

where $A = \lambda_i U_b \Delta x/k$ and $M = \rho c(\Delta x)^2/k\Delta t$ and is a dimensionless constant.

Equation 13 shows that the temperature of element i after time Δt is dependent on the initial temperatures T_{i-1}, T_i and T_{i+1}, together with the input of mechanical work, $\sigma_i d\varepsilon_i$. The coefficients of the initial temperatures when added together are equal to unity and the relative magnitude of a temperature coefficient gives an indication of the influence of the associated temperature on the new temperature, T'_i. Thus, the upstream temperature, T_{i-1}, at high drawing speeds is seen from Equation 13 to have a greater influence on T'_i than the downstream temperature, T_{i+1}. At low drawing speeds the magnitude of A is small and consequently T_{i+1} and T_{i-1} have approximately an equal effect on T'_i. The parameter M may be chosen arbitrarily but the chosen value determines the incremental time step during which temperature T_i increases to T'_i.

Equation 13 may be applied to all elements in the problem and the temperature distribution after time increment Δt evaluated throughout the die. The temperature after further time intervals can be determined from further iterations in which previously calculated temperatures become the initial temperatures in the new incremental step. A steady state temperature distribution is reached when iterations produce no significant increase in temperature of the elements.

Equation 12 allows for heat conduction in only one direction. Within the die a general element (Fig. 5b) will experience heat conduction in both the axial and radial directions and furthermore, the cross-sectional area through which the heat flows to adjacent radial and axial elements varies with element position. When Equation 13 is modified to take these factors into account it becomes

$$T'_{i,j} = T_{i+1,j}\left(Y - \frac{A\rho c}{2}\right)\Big/M + T_{i-1,j}\left(Z + \frac{A\rho c}{2}\right)\Big/M + T_{i,j+1}X/M + T_{i,j-1}W/M + T_{i,j}\left[\frac{M - (W + X + Y + Z)}{M}\right] + \frac{A\sigma_i d\varepsilon_i}{M} \quad (14)$$

where

$$W = \left(\frac{\Delta x_i}{\Delta y_{j-1}}\right)\left(\frac{a_{j-1}}{a_i}\right)\left(\frac{k_0}{k}\right)$$

$$X = \left(\frac{\Delta x_i}{\Delta y_{j+1}}\right)\left(\frac{a_{j+1}}{a_i}\right)\left(\frac{k_0}{k}\right)$$

$$Y = \left(\frac{\Delta x_i}{\Delta x_{i+1}}\right)\left(\frac{a_{i+1}}{a_i}\right)$$

$$Z = \left(\frac{\Delta x_i}{\Delta x_{i-1}}\right)\left(\frac{a_{i-1}}{a_i}\right)$$

The thermal conductivity in the radial direction was assumed to be constant and equal to the isotropic value but in the axial direction it is influenced by orientation and was assumed to be a function of position in the axial direction.

From the work of Greig and Sahota [22], thermal conductivity for polyethylene was taken as

$$k_i = 0.539\lambda_i - 0.110\ \mathrm{W\,m^{-1}\,K^{-1}} \quad (15)$$

The temperature rise due to mechanical work was determined assuming that all work is transformed into heat and thus the temperature rise in an element is given by

$$\Delta T = \frac{\sigma d\varepsilon}{c\rho} \quad (16)$$

6. Modelling the die-drawing process

The axial stress, σ_x, for any element in the die is dependent on the local flow stress (Equation 5) which, in turn, depends on the strain, strain rate and temperature within an element. To obtain a solution to the stress field within the die which takes into account the temperature rise due to the mechanical work of deformation, it was first necessary to determine the quasi-static temperature distribution from Equation 14 using a flow stress value for each element compatible with its temperature. This iterative calculation established the steady-state temperature and flow stress for each element and the axial stress could then be obtained from Equation 5 using finite difference techniques.

When obtaining a solution to the temperature distribution in the deforming polymer it was assumed that heat conduction occurred in the radial and axial directions and also through the die wall to the die which was maintained at the same constant temperature as the billet entering the die. At the die exit no heating was assumed to occur due to mechanical work and convection heat losses were assumed to be negligible.

The above computer model of the die-drawing process, detailed in Fig. 6, was used to study the behaviour of polyethylene homopolymer (BP grade R006-60) when drawn through a conical die having a 15° semi-die angle and 15.5 mm exit diameter. Dies having entrance diameters of 31 mm ($R_N = 4$) and 38 mm ($R_N = 6$) were evaluated for billet velocities of 5, 10 and 15 mm min^{-1} and a drawing temperature of 100 °C, which is in accordance with normal die drawing practice.

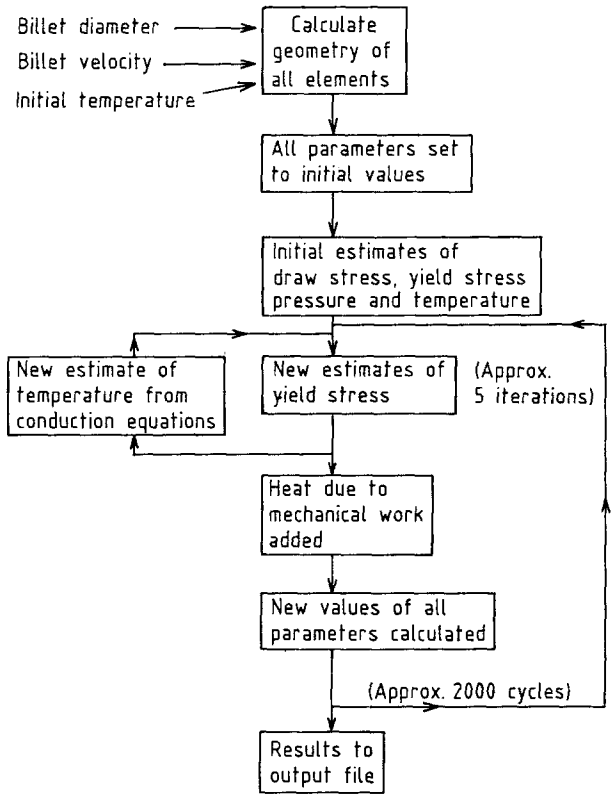

Figure 6 Flow chart of the computer model.

7. Results and discussion

A solution to the temperature field in the die was obtained for the above drawing conditions using Equation 14. It was found that for a stable converging solution, the temperature coefficients in Equation 14 had to be positive with, ideally, the coefficient of T_{ij} being dominant. To ensure that the coefficient of $T_{i+1,j}$ remained positive, parameter A, which is equal to $\lambda_i U_b(\Delta x_i)/k$, had to be kept small. An increase in drawing speed U_b had to be countered by a decrease in element size Δx_i, so increasing the number of axial slices used in the analysis. For the polyethylene billet and die-drawing conditions detailed above, the minimum number of axial slices required to keep the temperature coefficients positive, for various drawing speeds is shown in Table I.

For the solution to converge in a stable manner, the coefficient of T_{ij} had to be dominant and consequently

TABLE I Minimum number of slices needed for each die for various billet velocities

Billet velocity (mm min^{-1})	Number of slices needed for each die			
	$R_N = 4$	$R_N = 6$	$R_N = 8$	$R_N = 10$
2.5	7	13	19	27
5	13	24	38	53
7.5	19	36	56	79
10	25	48	74	105
12.5	32	60	92	131
15	38	72	112	158
17.5	44	84		
20	50	96		
25	63	120		
30	75	144		

parameter M, which is equal to $(\rho c/k)(\Delta x_i)^2/\Delta t$, had to be large. Temperature coefficient requirements as seen above, determined the magnitude of Δx_i so the only remaining independent variable which could be set to make M large, was time interval Δt. An acceptably large value of M was obtained when Δt was chosen such that about five iterations were required for an element of material to move downstream to the position of its neighbour. Under these conditions, the minimum number of iterative cycles required to obtain a steady state temperature distribution was five times the number of axial slices in the die and therefore this was equal to one complete pass of the material through the die. More passes made negligible difference to the final temperature distribution obtained.

7.1. Temperature distribution

Fig. 7 shows the calculated temperature distribution in polyethylene when drawn through the $R_N = 4$ die at various speeds. The plotted temperatures are surface temperatures but there was little difference between the centre and surface temperatures at any axial position in the die. The temperature profiles in Fig. 7 are remarkably similar due to the tension test flow stress data agreeing closely with those deduced by the Eyring activated rate theory. This close correlation shows that with a correct assessment of the stress activation volume, the Eyring theory is capable of modelling the yield behaviour of polymers undergoing the large-scale deformations of die drawing. At all draw speeds the mechanical work done produces a

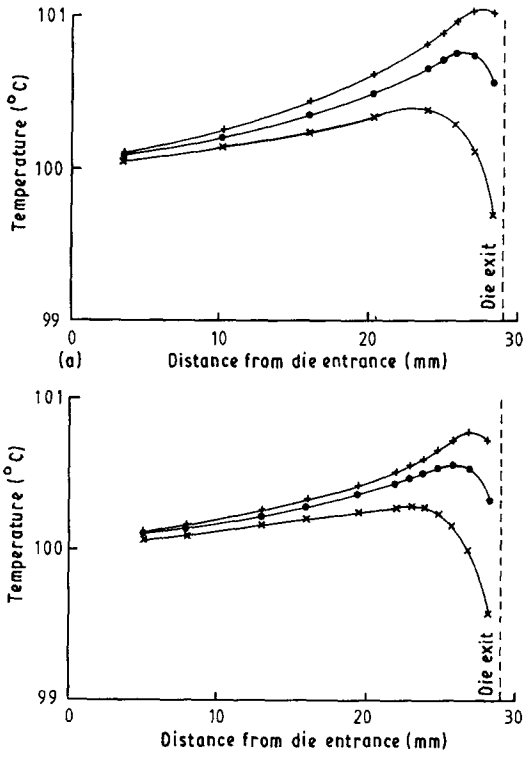

Figure 7 Calculated surface temperatures in polyethylene R006-60 when drawn through an $R_N = 4$ die at various billet velocities: (a) using activated rate theory, (b) using uniaxial tension test data; (×) 5 mm min^{-1}, (·) 10 mm min^{-1}, (+) 15 mm min^{-1}.

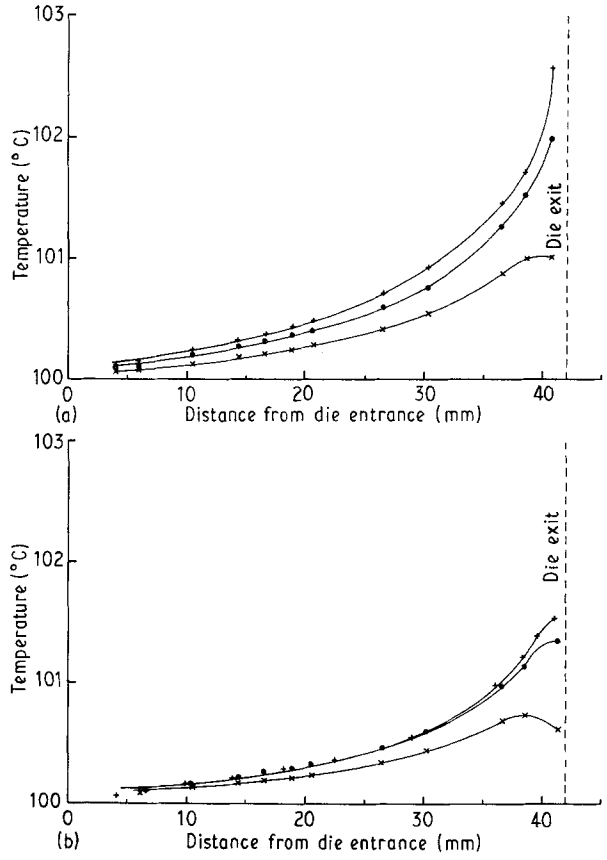

Figure 8 Calculated surface temperatures in polyethylene R006-60 when drawn through an $R_N = 6$ die at various billet velocities: (a) using activated rate theory, (b) using uniaxial tension test data; (×) 5 mm min^{-1}, (·) 10 mm min^{-1}, (+) 15 mm min^{-1}.

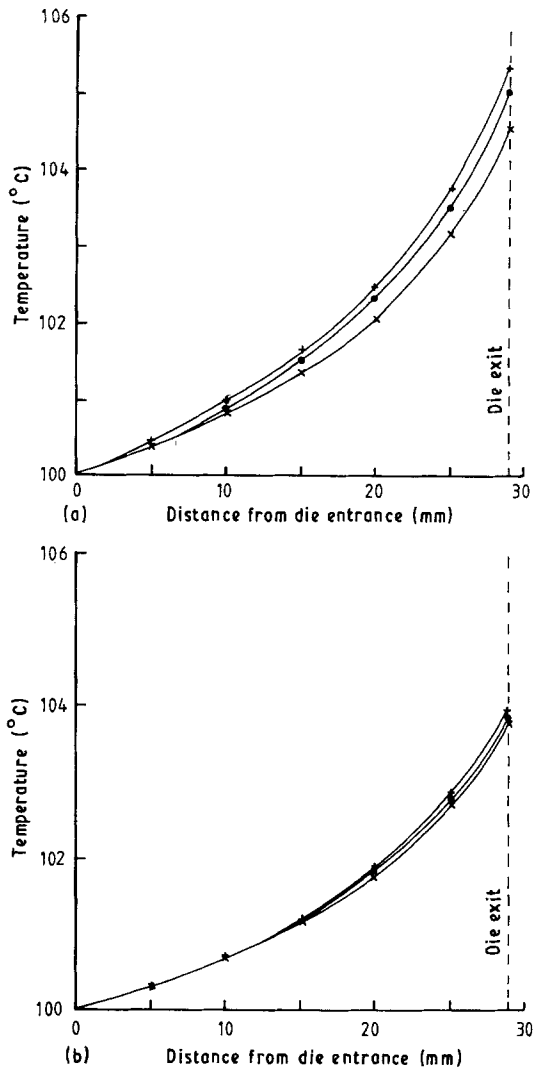

Figure 9 Calculated temperature rise in polyethylene R006-60 due to mechanical work alone when drawn through an $R_N = 4$ die, (a) using activated rate theory, (b) using uniaxial tension test data; (×) 5 mm min^{-1}, (·) 10 mm min^{-1}, (+) 15 mm min^{-1}.

rise in temperature which reaches a maximum near the die exit, but this maximum is only about 1° above the billet temperature for a billet speed of 15 mm min^{-1}. The fall in temperature near the die exit is due to the axial conduction of heat to material downstream of the die exit.

The temperature profile in the longer $R_N = 6$ die (Fig. 8) shows a pronounced upward trend near the die exit for billet speeds of 10 and 15 mm min^{-1}, whether calculated using uniaxial flow stress data or the activated rate theory. The increase in strain and particularly strain rate in the material as it approaches the die exit at the higher draw speeds, results in high flow stresses in this region and a consequent high generation of heat due to mechanical work. This high heat generation is significantly more important than the heat lost from the region by axial conduction and it accounts for the temperature rise in this region.

The temperature rise in the material due to mechanical work alone has been calculated for the various test cases using the expression

$$\Delta T = \int \frac{\sigma_i d\varepsilon_i}{c\rho} \qquad (17)$$

Figs 9 and 10 show the results obtained and when compared with those in Fig. 7, where heat conduction and axial translation are taken into account, it can be seen that these latter factors significantly reduce temperatures produced by mechanical work alone. Figs 9 and 10 have been calculated using flow stress values obtained from activated rate theory and from tensile data and these figures show the final temperature reached in the $R_N = 6$ die is significantly greater than that in the $R_N = 4$ die, with billet velocity having little influence on temperature over the range of velocities investigated.

7.2. Flow stress

The computer model was used to determine the flow stress within the $R_N = 4$ and $R_N = 6$ dies, taking into account strain, strain rate and temperature. Figs 11 and 12 show values of flow stress relating to die surface elements for any axial position within the dies. Although axial slices only were used to establish the quasi-static equilibrium relationships within each die, temperatures were determined using both axial and radial elements and hence it was appropriate to determine centre and surface yield stress values throughout the dies.

Figs 11 and 12 both show the surface flow stress predicted by activated rate theory to be similar to that obtained from tension data at the die entrance but the difference in flow stress between the two approaches,

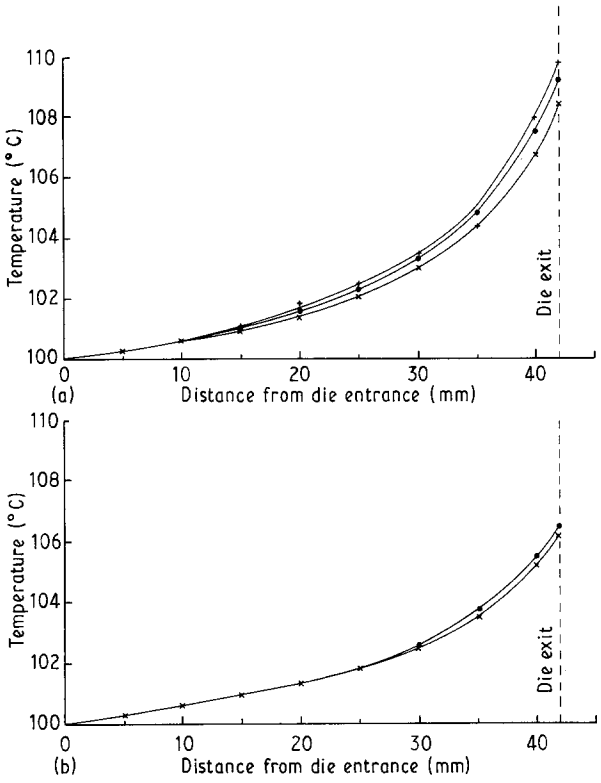

Figure 10 Calculated temperature rise in polyethylene R006-60 due to mechanical work alone when drawn through an $R_N = 6$ die, (a) using activated rate theory, (b) using uniaxial tension test data; (×) 5 mm min^{-1}, (·) 10 mm min^{-1}, (+) 15 mm min^{-1}.

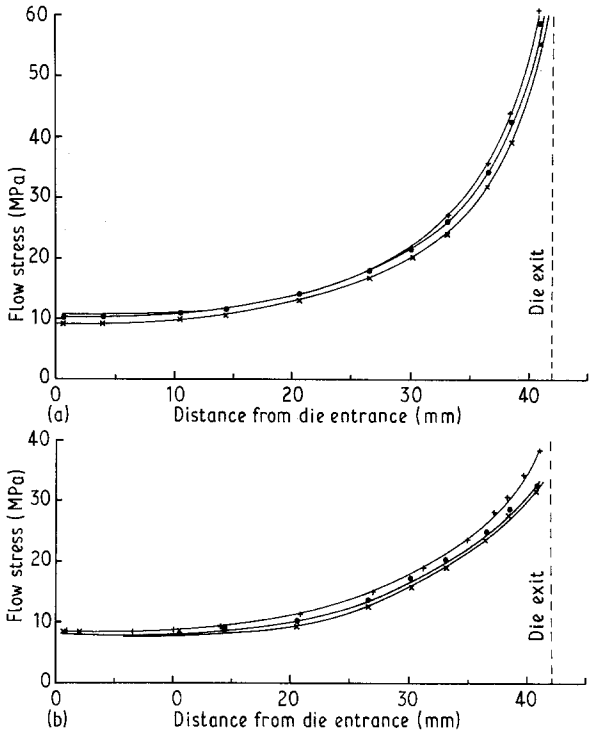

Figure 12 Flow stress in elements of polyethylene R006-60 drawn through an $R_N = 6$ die at various billet velocities, (a) using activated rate theory, (b) using uniaxial tension test data; (×) 5 mm min^{-1}, (·) 10 mm min^{-1}, (+) 15 mm min^{-1}.

increases with position along the die and is greatest at the die exit. For the range of velocities investigated the flow stress is found to be not markedly dependent on billet velocity.

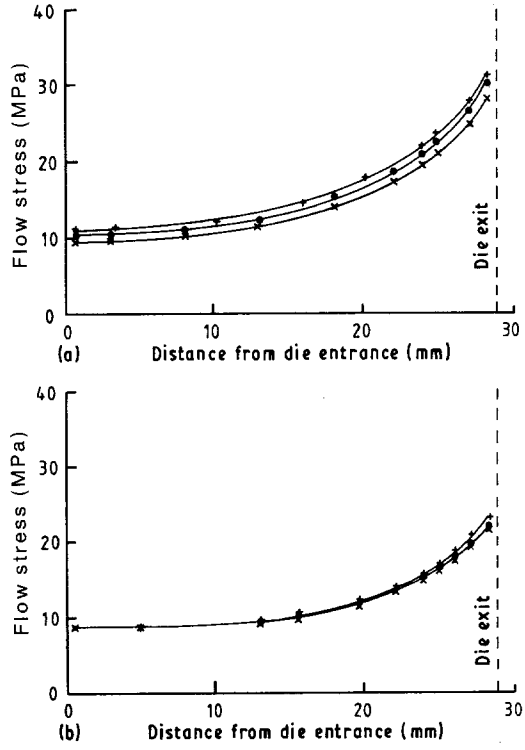

Figure 11 Flow stress in elements of polyethylene R006-60 drawn through an $R_N = 4$ die at various billet velocities, (a) using activated rate theory, (b) using uniaxial tension test data; (×) 5 mm min^{-1}, (·) 10 mm min^{-1}, (+) 15 mm min^{-1}.

7.3. Axial stress and die-wall pressure

The axial stress in the $R_N = 4$ and $R_N = 6$ dies was obtained using the computer model and the results are shown in Figs 13 and 14. For the $R_N = 4$ die (Fig. 13), the axial stresses derived using activated rate theory are slightly greater than those derived from tension data with billet velocity having little influence on these stresses. Similar behaviour is seen in Fig. 14 for the $R_N = 6$ die and axial stress in both dies shows an upward trend towards the die exit, similar to the flow stress behaviour in the dies. The flow stress is equal to the difference between the axial stress, σ_x, and the die-wall pressure, p (Equation 4), if these stresses are assumed to be principal stresses, which is essentially true provided friction effects in the die and the die semi-angle are both small. Figs 15 and 16 show that the die-wall pressures, particularly near to die exit, are relatively small and consequently the axial stress is greatly influenced by the flow stress characteristics of the material.

The die-wall pressure (Figs 15 and 16) reaches a minimum value near to the die exit. Polymers have been observed to leave the die wall in this region so that the die wall pressure at such points will be equal to zero. Polyethylene in this investigation will not exhibit this behaviour due to the die-wall pressure remaining positive throughout the die.

7.4. Experimental draw stress data

Richardson *et al.* [13] have carried out die-drawing tests using polyethylene R006-60 billets having the same size and drawn under the same conditions as

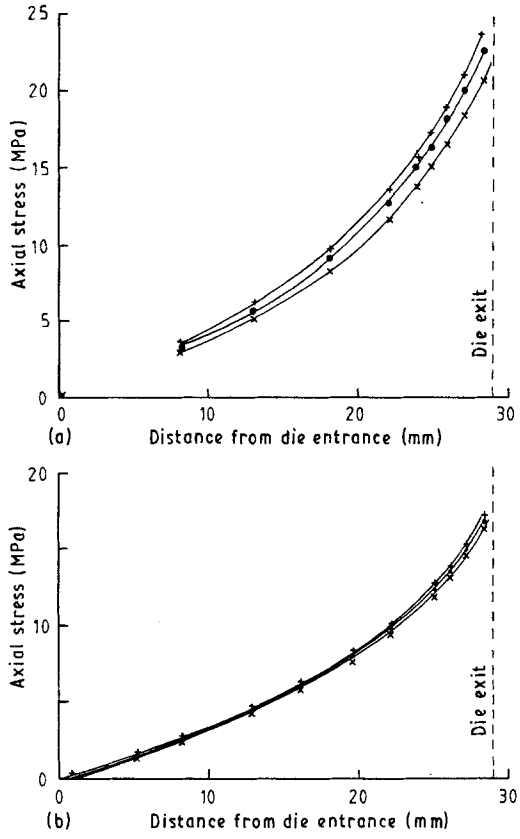

Figure 13 Axial stress on polyethylene R006-60 elements when drawn through an $R_N = 4$ die at various billet velocities, (a) using activated rate theory, (b) using uniaxial tension test data; (×) 5 mm min^{-1}, (·) 10 mm min^{-1}, (+) 15 mm min^{-1}.

assumed in this theoretical investigation. Temperature, flow stress and die-wall pressure in the die could not be measured in the drawing tests but drawing stress results for the die exit can be compared with

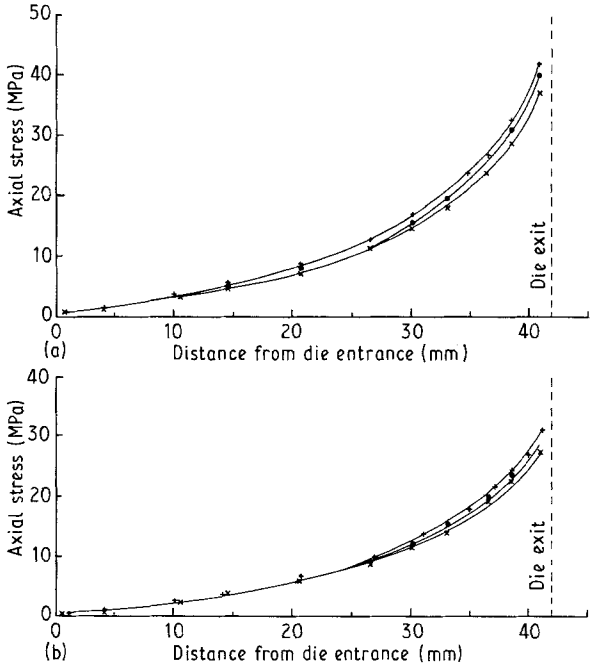

Figure 14 Axial stress on polyethylene R006-60 elements when drawn through an $R_N = 6$ die at various billet velocities, (a) using activated rate theory, (b) using uniaxial tension test data; (×) 5 mm min^{-1}, (·) 10 mm min^{-1}, (+) 15 mm min^{-1}.

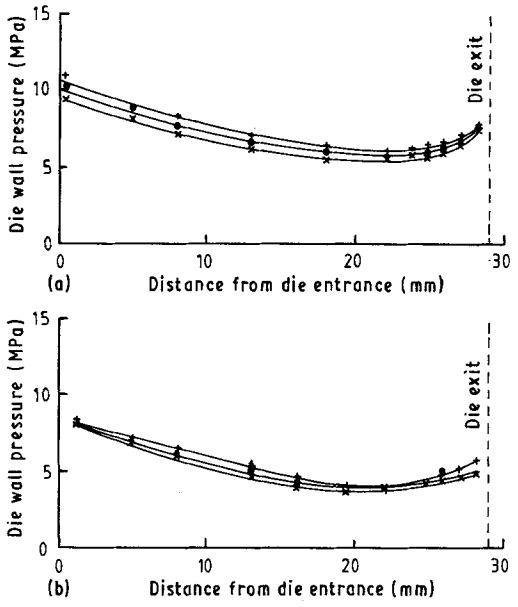

Figure 15 Die-wall pressure when drawing polyethylene R006-60 through an $R_N = 4$ die at various billet speeds, (a) using activated rate theory, (b) using uniaxial tension test data; (×) 5 mm min^{-1}, (·) 10 mm min^{-1}, (+) 15 mm min^{-1}.

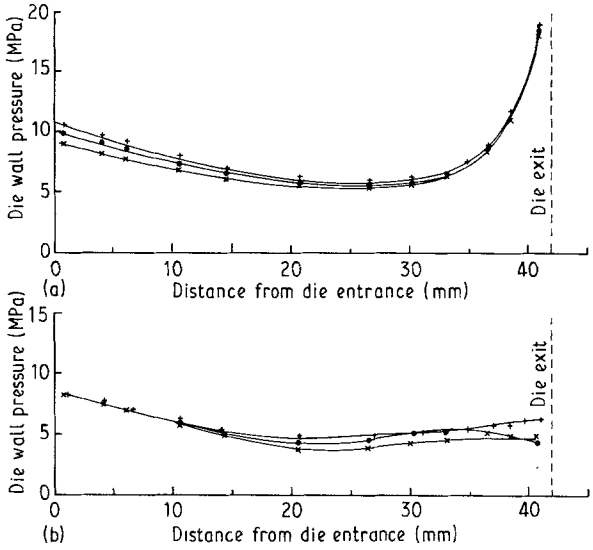

Figure 16 Die-wall pressure when drawing polyethylene R006-60 through an $R_N = 6$ die at various billet speeds, (a) using activated rate theory, (b) using uniaxial tension test data; (×) 5 mm min^{-1}, (·) 10 mm min^{-1}, (+) 15 mm min^{-1}.

theoretical values. Fig. 17 shows that for the $R_N = 4$ die the experimental draw stress results show good agreement with the activated rate theory predictions at low haul-off speeds but at the higher speeds the computer model results are approximately 20% less than those determined experimentally. The $R_N = 6$ activated rate theory results show very close agreement with experimental behaviour over the range of velocities investigated. Tensile test data results, however, predict consistently lower draw stress values than found experimentally.

8. Conclusions

1. It is possible to analyse the die-drawing behaviour of polyethylene in the solid phase by modelling the

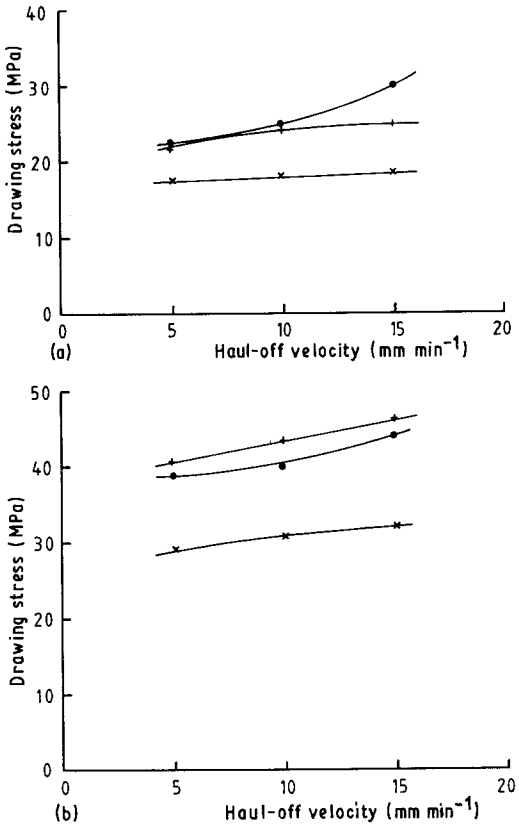

Figure 17 Comparison of (·) experimental and calculated values of drawing stress using (+) activated rate theory and (×) uniaxial tension data. (a) Die having $R_N = 4$, (b) die having $R_N = 6$.

mechanics, physics and heat conduction effects during drawing.

2. A single-process activated rate theory model adequately described the flow stress behaviour of polyethylene.

3. A method has been successfully developed for obtaining true stress–strain data at constant true strain rate from mechanical tests and applying such data to the model.

4. The temperature distribution in the dies has been determined taking into account heat conduction and axial translation of the material within the die. Temperatures in the die are substantially lower than those predicted from estimates using the mechanical work done within the die, and assuming that there are no heat losses for any reason.

5. Strain rate and temperature within the die have a marked influence on the flow stress which primarily determines the drawing behaviour of polyethylene. Predicted values of the draw stress using the activated rate theory model show good agreement with experimental values.

Acknowledgements

We thank the Polymer Engineering Group of the Science and Engineering Research Council for financial support. The help of Professor B. Parsons, Queen Mary College, in the early stages of this work is also gratefully acknowledged.

References

1. G. CAPACCIO and I. M. WARD, *Nature (Phys. Sci.)* **243** (1973) 143; *Brit. Pat. Appl.* 10746/73 (1973).
2. *Idem., Polymer* **15** (1974) 233.
3. *Idem., Polym. Engng Sci.* **15** (1975) 219.
4. A. G. GIBSON and I. M. WARD, *Brit. Pat. Appl.* 30823/73 (1973).
5. A. G. GIBSON, I. M. WARD, B. N. COLE and B. PARSONS, *J. Mater. Sci.* **9** (1974) 1193.
6. I. M. WARD, *Adv. Polym. Sci.* **70** (1985) 1.
7. P. D. COATES and I. M. WARD, *Polymer* **20** (1979) 1553.
8. A. G. GIBSON and I. M. WARD, *J. Mater. Sci.* **15** (1980) 979.
9. *Idem., Polym. Engng Sci.* **20** (1980) 1229.
10. P. S. HOPE, A. RICHARDSON and I. M. WARD, *J. Appl. Polym. Sci.* **26** (1981) 2879.
11. A. RICHARDSON, P. S. HOPE and I. M. WARD, *J. Polym. Sci. Phys. Ed.* **21** (1983) 2525.
12. A. RICHARDSON, F. ANIA, D. R. RUEDA, I. M. WARD and F. BALTA CALLEJA, *J. Polym. Engng Sci.* **25** (1985) 355.
13. A. RICHARDSON, B. PARSONS and I. M. WARD, *Plastics Rubber Proc. Appl.* **6** (1986) 347.
14. I. M. WARD, A. SELWOOD, B. PARSONS and A. GRAY, "Plastics Pipes VI" (Plastics and Rubber Inst., York, 1985).
15. O. HOFFMAN and G. SACHS, "Introduction to the Theory of Plasticity for Engineers" (McGraw-Hill, New York, 1953).
16. S. GLASSTONE, K. LAIDLER and H. EYRING, "The Theory of Rate Processes" (McGraw-Hill, New York, 1941).
17. B. AVITZUR, "Metalforming: Process and Analysis" (McGraw-Hill, New York, 1968).
18. P. D. COATES, A. G. GIBSON and I. M. WARD, *J. Mater. Sci.* **15** (1980) 359.
19. P. D. COATES and I. M. WARD, *J. Mater. Sci.* **13** (1978) 1957.
20. P. S. HOPE and I. M. WARD, *ibid.* **16** (1981) 1511.
21. I. M. WARD, "Mechanical Properties of Solid Polymers", 2nd Edn (Wiley, Chichester, 1983) Chs 7 and 9.
22. D. GREIG and M. SAHOTA, *Polymer* **19** (1978) 503.
23. H. CARSLAW and J. C. JAEGER, "Heat Conduction in Solids" (Clarendon, Oxford, 1958).

Received 13 June
and accepted 1 July 1991